

Physicochemical characterisation of novel ultra-thin biodegradable scaffolds for peripheral nerve repair

Mingzhu Sun · Sandra Downes

Received: 18 September 2008 / Accepted: 15 December 2008 / Published online: 10 January 2009
© Springer Science+Business Media, LLC 2009

Abstract In this study, the physicochemical properties of microporous poly (ϵ -caprolactone) (PCL) films and a composite material made of PCL and polylactic acid (PLA) blend were tested. Fabricated by solvent casting using dichloromethane, these ultra-thin films ($60 \pm 5 \mu\text{m}$ in thickness) have a novel double-sided surface topography, i.e. a porous surface with pores $1\text{--}10 \mu\text{m}$ in diameter and a relatively smooth surface with nano-scaled texture. Porous surfaces were found to be associated with increased protein adsorption and the treatment of these polyester scaffolds with NaOH rendered them more hydrophilic. Differential Scanning Calorimetry (DSC) showed that the incorporation of PLA reduced the crystallinity of the original homopolymer. Chemical changes were investigated by means of Fourier Transform Infrared Spectroscopy (FTIR) and X-ray photoelectron spectroscopy (XPS). Average surface roughness (Ra), hydrophilicity/hydrophobicity and mechanical properties of these materials were also assessed for the suitability of these materials as nerve conduits.

1 Introduction

Peripheral nerve trauma, with an estimated incidence of 1 in 1000 of the general population per year [1] and 300,000 cases annually in Europe [2], remains a major cause of morbidity and clinical need. Currently, the preferred repair method is an autologous nerve graft to span the injury site;

however, this is far from an optimal treatment due to the extra damage to the donor site, scarring, neuroma formation and poor sensory function recovery [3].

Recent efforts in peripheral nerve regeneration have been directed towards the development of slowly resorbable artificial nerve guides. Advantages of tubular nerve guidance include providing mechanical support, confining intrinsic growth factors in situ, preventing neuroma formation and minimizing infiltration of fibrous tissue [2, 4].

Numerous natural and synthetic materials have been tested as scaffold for nerve repair [5, 6]. One promising material is poly (ϵ -caprolactone) (PCL), which is U.S. Food and Drug Administration (FDA) approved for hard- and soft-tissue repair [7, 8]. PCL, a semicrystalline polyester, has a low glass-transition temperature (T_g) of -60°C , a melting point of 60°C , and a high decomposition temperature of 350°C [9]. The aliphatic ester linkage in PCL is susceptible to hydrolysis in vivo and the break-down products generated can be either metabolized via the tricarboxylic acid cycle or eliminated directly by renal secretion [10, 11].

Although degradation rate depends on the size, molecular weight and crystallinity of the scaffold, PCL is a slow degrading material which takes of the order of 24 months to break down [12]. Whereas the maturation over a 1 cm gap in the sciatic nerve of the rat takes place within 16 weeks [13]. Poly (lactic acid) (PLA), a fast degrading amorphous racemic mixture of D and L isomers, was therefore incorporated to make a polymer-blend with PCL. PLA is another FDA approved biodegradable polyester. However, the poor mechanical properties and fast degradation of PLA in vivo made it unsuitable for long-term clinical applications. It has been reported that the mechanical properties of PCL/PLA can be tuned through the blend composition and the ultimate tensile strength can be continuously varied by an order of magnitude [14]. PCL can also lower the elastic modulus

M. Sun · S. Downes (✉)
Materials Science Centre, Department of Engineering
and Physical Sciences, The University of Manchester,
Grosvenor Street, Manchester M1 7HS, UK
e-mail: sandra.downes@manchester.ac.uk

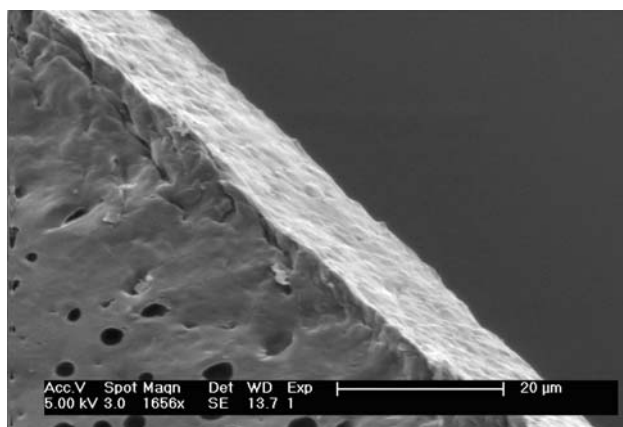


Fig. 1 SEM image showing the cross-section of the PCL/PLA blend film. The film was cast onto $18 \times 18 \text{ mm}^2$ glass coverslips with a thickness of approximately $16 \mu\text{m}$. No phase separation between PCL and PLA was evident

and soften the other polymers when used in blends [15, 16]. By combining PCL and PLA together, the merits of both polymers could possibly be retained and at the same time the problems avoided.

It has been noticed that poly (L-lactide)(PLLA)/PCL blends suffer from poor mechanical properties due to macro phase separation of the two immiscible components and poor adhesion between phases [17]. Whereas when amorphous PLA was used to make the blend with a majority of PCL, some adhesion may occur at the interface [14]. In addition, Wang et al. [18] showed that some kinds of synergism exist at certain compositions (PLA/PCL = 80/20, 20/80). Our SEM imaging at the cross-section of the ultra-thin PCL/PLA film showed no evident phase separation (Fig. 1).

The aim of this research was to investigate the suitability of the solvent casting method in fabricating an ultra-thin film that had the desirable physicochemical properties to be used as a nerve conduit.

2 Materials and methods

PCL ($M_n \sim 80,000 \text{ g/mol}$) and PLA ($M_n \sim 30,000 \text{ g/mol}$), a racemic mixture of D and L isomers, were purchased from Sigma-Aldrich. Dichloromethane (CH_2Cl_2) was from Fisher Scientific. Poly (3-hydroxybutyrate) (PHB; MW $\sim 63,500 \text{ g/mol}$) was from Astra Tech, Sweden. Bicinchoninic Acid Protein Assay Kit was from Sigma-Aldrich.

2.1 Preparation of the PCL and PCL/PLA blend films

PCL pellets were dissolved in dichloromethane (3% wt/v). Gentle heating in a water bath at a temperature of

approximately 50°C was carried out to assist dissolving. Fully dissolved and equilibrated PCL solutions were evenly cast onto a borosilicate glass coverslip ($18 \times 18 \text{ mm}^2$ or $75 \times 25 \text{ mm}^2$), which had been degreased with acetone/ethanol (1:1, v/v). Films were left to dry in a well ventilated lab atmosphere at room temperature. Complete solvent evaporation was allowed in a fume cupboard for at least 48 h. The polymer films were then washed in distilled H_2O and sterilized by UV irradiation for 1 h prior to cell culturing. A PCL/PLA polymer blend consisting of a mixture of PCL and PLA (ratio = 4:1 w/w) was prepared using the same method.

2.2 Surface modification using NaOH

Films prepared as described above were soaked in 10 N NaOH for 1 h with gentle shaking at room temperature, and then rinsed thoroughly with distilled H_2O to return the pH to neutral (pH 7.2–7.4). Basic hydrolysis introduces random scission to the polyester chains and produces free $-\text{COOH}$ and $-\text{OH}$ groups, which will make the materials more hydrophilic.

2.3 PLA and PHB comparative films

For the purpose of direct comparison, PLA films were fabricated using the same method as that for PCL and the composite films. PHB mats were dissolved into chloroform at 70°C and cast onto the surface of glass slides as described above. PHB was included in this study as a comparison because it is an extensively studied material in peripheral nerve repair with many desirable properties [19]; however, nerve regeneration in PHB conduits was moderate even with the addition of fibrin matrix and Schwann cells/differentiated mesenchymal stem cells [20]. Neither PLA films nor PHB films could withstand NaOH treatment, and both broke into small pieces.

2.4 Chemical analysis

ATR-FTIR spectra of the samples were generated by a Thermo Nicolet NexusTM FTIR (Cambridge, UK) controlled by OMNIC software Version 6.1a. Briefly, the films were mounted onto a SMART OMNI-Sampler connected to the FTIR Nexus. The machine was operated under the experiment ATR-GE and the spectra were obtained by accumulating 32 scans in the range $600\text{--}4000 \text{ cm}^{-1}$ with a resolution of 4 cm^{-1} .

X-ray photoelectron spectroscopy (XPS) (AXIS Ultra) was used to detect variations in chemical composition, oxidation state and electronic state of the elements existing within a material. A survey scan spectrum was taken and surface elemental stoichiometries were determined from

peak-area ratios. Data was processed and spectra generated using CasaXPS software.

2.5 Thermal analysis

Differential Scanning Calorimetry (DSC, Q100 V9.8) was used to analyze the thermal properties of the solvent-cast polymer films. Samples were sealed hermetically in aluminium pans and heating was carried out in the range of -70°C to 150°C with a heating rate of $20^{\circ}\text{C}/\text{min}$. The measurement was carried out at a scanning rate of $10^{\circ}\text{C}/\text{min}$ and nitrogen gas flow rate of $50\text{ ml}/\text{min}$. The TA Instruments Universal Analysis 2000 software (Version 4.4A) was used for the data analysis.

Percentage crystallinity was calculated from the heat of fusion using a 100% crystalline poly (ϵ -caprolactone) as a reference, which has a fusion enthalpy of $135.44\text{ J}/\text{g}$. This calculation is based on the proportionality of heat of fusion and the experimental enthalpy [21].

2.6 Mechanical strength of PCL and the PCL/PLA blend films

Tensile strength and Young's modulus were measured on a mechanical tensile tester (Instron 1122) at $23 \pm 1^{\circ}\text{C}$ temperature, $50 \pm 2\%$ relative humidity. A crosshead speed of $50\text{ mm}/\text{min}$ was used and the cross area was $(3.8 \times 0.06)\text{ mm}^2$. The grip distance was 35 mm and the full scale load was set at 0.005 KN . Young's modulus was measured from the initial slopes in the elastic region and the tensile strength was the average of ultimate stress at the breaking point of the films.

The thickness of PCL films was measured using an Electronic Digital Outside Micrometer (Roebuck). Five randomly selected areas were measured on each of ten films. Porosity was measured on SEM images using the Image J software. Twenty randomly selected areas ($50 \times 50\text{ }\mu\text{m}^2$) were measured for each sample and the average values were used.

2.7 Wettability testing

Hydrophilicity/hydrophobicity was compared by measuring the static water contact angles using a Krüss DSA 100 Drop Size Analyser. Five treated or untreated films were tested and five randomly selected areas were measured.

2.8 AFM and SEM surface analysis

Atomic Force Microscopy (AFM, Veeco CP2) and Field Emission Gun Scanning Electron Microscopy (FEG-SEM, Philips XL30) techniques were used to obtain information

about the surface topography. A scanning frequency of approximately 0.4 kHz was used in contact mode.

Surface roughness and pore size were measured using IP Image Analysis 2.1 software on images taken with AFM.

2.9 Protein adsorption analysis

DMEM cell culture medium containing 50% of foetal bovine serum was used to soak the materials for 30 min at room temperature. Films were washed twice in PBS and the Bicinchoninic Acid Protein Assay Kit (BCA assay) was used to detect the absorbed proteins according to the standard protocol with the ratio of reagent A and reagent B at 50:1. Films were incubated at room temperature overnight. About $200\text{ }\mu\text{l}$ of each sample solution was added into a 96-well plate and the absorbance was read at 540 nm on a microplate reader (LabSystem, Multiskan, Ascent).

2.10 Statistical analysis

The SPSS statistical program (version 14.0) was used to perform statistical analyses. Independent Sample *T* Test was used to determine the statistical significance amongst different samples in wettability, tensile strength, Young's modulus, protein adsorption and average surface roughness. Statistical significance before and after NaOH treatment was determined using Paired-Sample *T* test. $*P < 0.05$ was regarded as significant.

3 Results

Initially, PCL and PCL/PLA solutions in a series of concentrations (wt/v) (0.5%, 1.5%, 3.0%, 4.5% and 10%) were tested. Only films fabricated using solutions of 3.0% concentration were analyzed in this study, which exhibited best flexibility and mechanical strength for processing and handling.

3.1 Complete solvent evaporation and chemical stability

FTIR analysis showed that no chemical changes occurred during the solvent casting procedure and no residue solvent remained in the tested sample films. This was based on the spectra (data not shown) constructed from the FTIR data, which showed no peak shift between the films and the raw material. However, no peaks representing the $-\text{COOH}$ group and the $-\text{OH}$ group could be detected. No peaks representing the chemical bonds in dichloromethane were found in the spectra of the PCL films, indicating complete solvent evaporation. Complete solvent removal is the principal problem arising in the context of the fabrication

of polymer films by solution casting. This is because of the possible toxic effects in the use of the materials as implants; additionally the remaining solvents can act as a plasticizer and falsify the analysis of mechanical properties [22].

3.2 Hydrolysis of ester bonds

Ester bonds in polyesters, such as poly (ϵ -caprolactone), are subject to hydrolysis in basic solutions. XPS data confirmed the chemical change before and after NaOH treatment. The O 1s peak shape clearly distinguishes the two chemical environments of O (oxygen) present in the polymer. Furthermore, the high energy resolution allowed unambiguous curve fitting of the O 1s region to determine the amount of C–O groups and C=O groups present at the surface of the film. Before NaOH treatment, there was approximately an equal amount of C–O groups and C=O groups (Fig. 2, left panel). However, the treatment generated free –COOH groups and –OH groups by partially hydrolyzing the polymer resulting in a reduced amount of C–O groups on the surface of the polymer (Fig. 2, right panel).

3.3 Ultra thin film

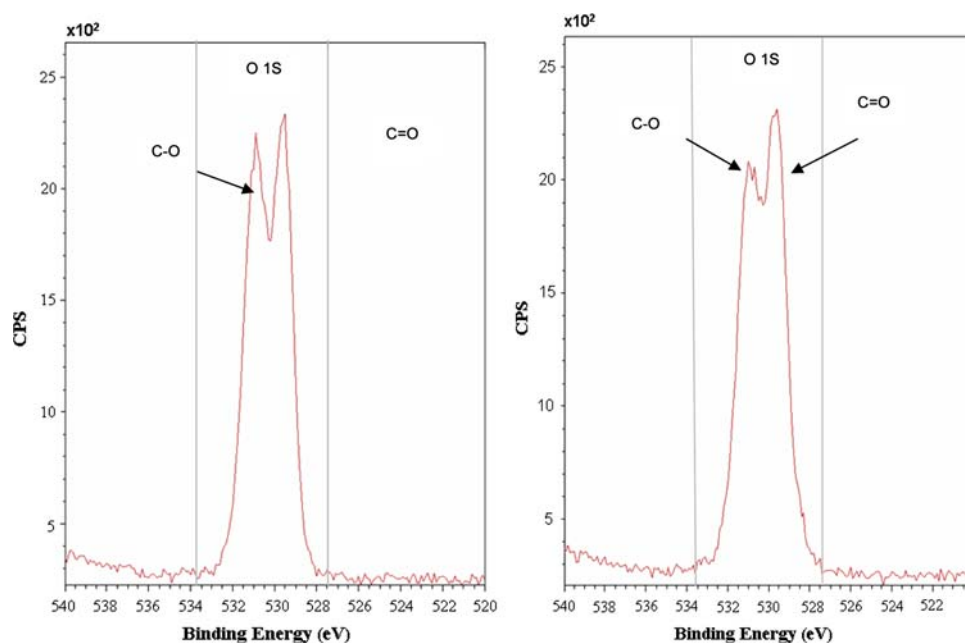
An average thickness of $60 \pm 5 \mu\text{m}$ was measured for PCL and PCL/PLA films ($75 \times 25 \text{ mm}^2$) made from 4 ml of 3% solution, which is much smaller than normal films produced for nerve repair. PCL and PCL/PLA films cast on $18 \times 18 \text{ mm}^2$ glass coverslips had a thickness of $15.9 \pm 1.8 \mu\text{m}$.

3.4 Micro-porous air surface and nano-porous glass surface

Due to the nature of the casting method, both PCL and PCL/PLA films had two surfaces: namely, an air surface and a glass surface. SEM and 3-D AFM images revealed that dichloromethane cast PCL films were micro-porous with pores on the air surface in the range of 1–10 μm in diameter, the mean value being 5.76 μm . The depth of these pores was between 1 and 5 μm , mean value 1.96 μm (Figs. 3a, 4a). The glass surface was also porous with pores in the diameter of 1–5 μm . However, the depth of pores on this side of the films was down to 100–800 nm (Figs. 3b, 4b). Due to the air-flow and/or other factors unknown currently, the films have some penetrating holes of diameter 10–25 μm , which will enable the exchange of metabolites between the conduit lumen and the surrounding tissues. Apart from these large holes, the pores in the majority area of the films were blind-ended pits. The percentage of large holes was less than 5% of the total surface area (Fig. 3, inset).

PCL/PLA polymer blend films were also micro-porous at the air surface. However, the diameter of pores on PCL/PLA films was in the range of 1–8 μm , mean value being 3.96 μm . The depth of these pores fell in the range of 0.5–3 μm , mean value 1.63 μm (Fig. 5a). The glass surface of PCL/PLA films has a similar texture as that of PCL films with pore size in the range of 1–3 μm and a nano-scaled depth between 100 and 500 nm. PLA films and PHB films prepared in this work were also porous with pore size smaller than 5 μm (data not shown). After NaOH treatment, some nano-scaled pits appeared at the air surface of

Fig. 2 XPS spectra for dichloromethane cast PCL films before (left panel) and after (right panel) NaOH treatment. NaOH treatment breaks the ester bonds on the polymer chains and generates free –COOH and –OH groups. Before NaOH treatment, the amount of C=O groups and C–O groups was similar. After NaOH treatment, the reduced peak of C–O groups proved the occurrence of alkaline hydrolysis



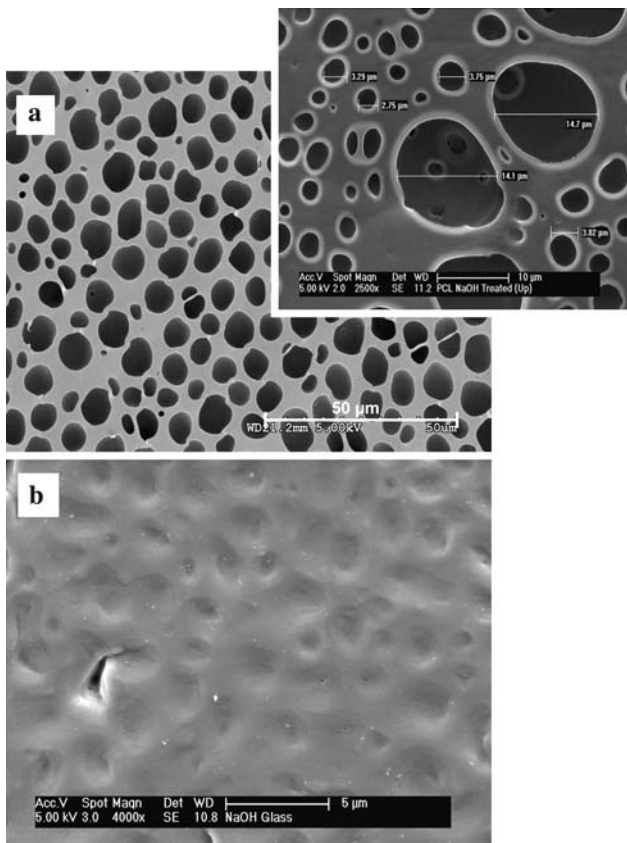


Fig. 3 SEM images of dichloromethane cast PCL films. **a** Microporous air surface. **b** Glass surface with nano-texture. SEM imaging revealed that PCL films were microporous with pores on the air surface in the range of 1–10 μm in diameter, the depth of these pores was between 1 and 5 μm. The glass surface was also porous with pores of diameter 1–5 μm. However, the depth of pores on this side of the films was down to 100 nm–800 nm. Inset shows larger pores of diameter 10–20 μm. These were penetrating pores allowing metabolites exchange (bar = 10 μm)

the PCL/PLA films (Fig. 5b), which was not observed on NaOH treated PCL homopolymer films.

The porosity of PCL, PLA and PCL/PLA films is listed in Table 1, which shows that PCL has the highest porosity (51%) amongst these three samples, PCL/PLA the lowest (35.8%) and PLA in the middle (45.2%).

3.5 The effect of NaOH treatment

It can be observed from the data shown in Table 2 that the static water contact angle on the glass surface of the polymer films was smaller than that on the air surface. It should be noted that other factors, e.g. surface roughness can affect the wettability of materials with the same chemical composition [23]. The rougher porous air surface was expected to have a higher water contact angle than the smooth glass surface. The NaOH treated surfaces (both air

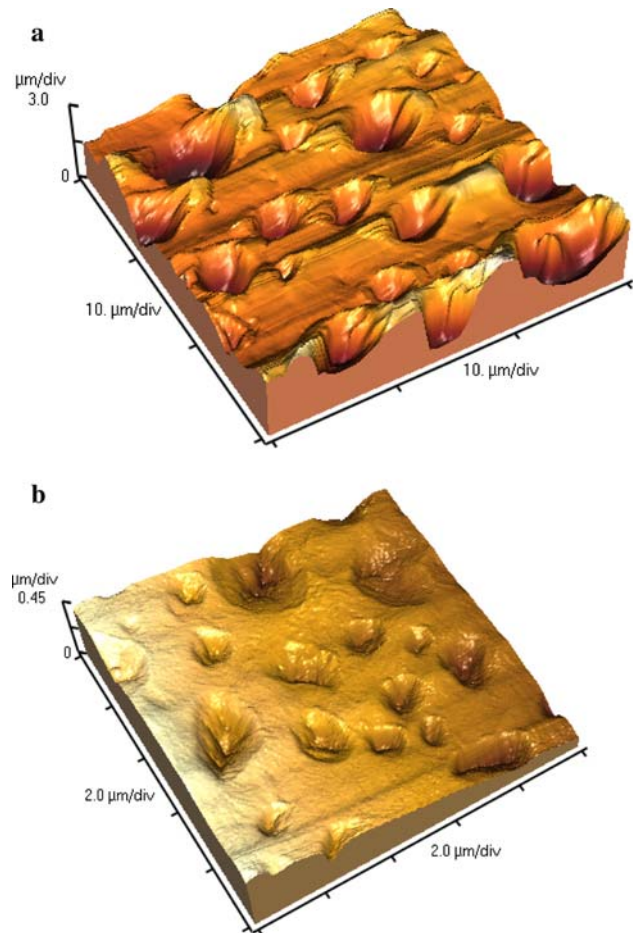


Fig. 4 3-D AFM image of the dichloromethane cast PCL films. **a** Air surface, scanned area is 30 × 30 μm². **b** Glass surface of PCL film, scanned area is 10 × 10 μm². It was observed that the pores on both sides of the films were blind-ended

surface and glass surface) of the PCL films were significantly more hydrophilic than the untreated counterparts; whereas the difference between NaOH treated and untreated PCL/PLA blend films was not significant. The high standard deviations were considered to be resulted from the preferential hydrolysis of the amorphous areas of the polymer films against the crystalline areas [24]. The manual fabrication of the materials was also believed to be the cause of high standard deviations. The PCL/PLA composite materials had significantly poorer hydrophilicity than scaffolds made of PCL homopolymer both before and after the NaOH treatment. PLA and PHB films had significantly poorer wettability when compared with untreated PCL films.

NaOH treatment reduced the average surface roughness (Ra) on the air surface of the films by nanometres, from 3.883 μm to 3.041 μm (842 nm) for PCL films and 3.39 μm to 2.455 μm (935 nm) for PCL/PLA films, respectively. As for the glass surface of the materials,

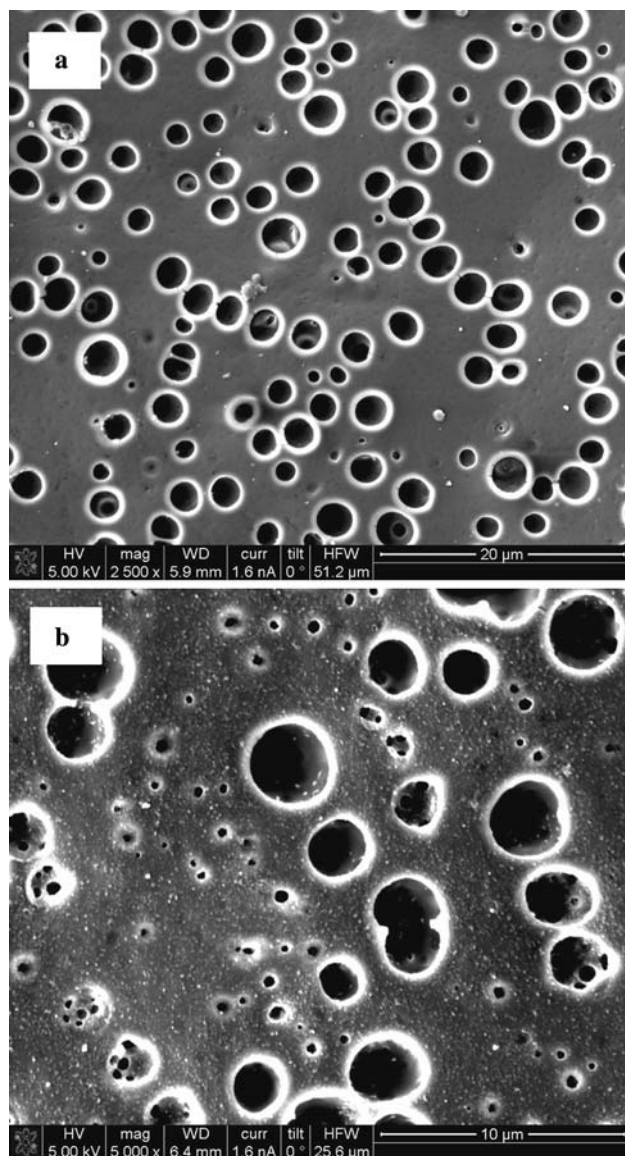


Fig. 5 Dichloromethane cast PCL/PLA films. **a** Before NaOH treatment. **b** After NaOH treatment. The PCL/PLA blend films were less porous (35.8%) than the PCL homopolymer films (51%) and the size of the pores was also smaller (1–8 μm). NaOH treatment generated nano-scaled feature on the surface

Table 1 Porosity of different materials

Materials	Porosity (% of total surface area)
PCL	51.0
PLA	45.2
PCL/PLA	35.8

Measured using Image J software. (Twenty randomly selected areas were measured and the size of the individual area was $50 \times 50 \mu\text{m}^2$)

NaOH did not significantly affect the surface roughness. Pore size stayed unchanged before and after the NaOH treatment.

Table 2 Static water contact angle for PCL films, NaOH treated PCL films, PCL/PLA films and NaOH treated PCL/PLA films

Samples	Water contact angle ($^\circ$) mean value	Standard deviation ($^\circ$)
PCL-OH-G	36.7	4.65
PCL-OH-A	52.79	10.8
PCL-G	43.81	6.3
PCL-A	64.58	2.8
PCL/PLA-OH-G	61.49	4.6
PCL/PLA-OH-A	74.45	9.2
PCL/PLA-G	69.36	4.2
PCL/PLA-A	76.63	6.5
PLA-A	71.33	3.3
PHB-A	80.03	1.8

PLA and PHB films were included as comparison. ‘-OH’ denotes NaOH treatment; ‘G’ designates glass surface; ‘A’ porous/pitted air surface

3.6 Mechanical properties of PCL and PCL/PLA films

Tensile strength (represented by Max. STR.) of the films made from the PCL/PLA composite polymer was significantly lower than that of the PCL films alone (Table 3), whereby a reduced degradation rate can be expected. NaOH treatment also reduced the tensile strength of both PCL films (from 16.3 ± 3.97 MPa to 14.98 ± 2.77 MPa) and the PCL/PLA films (from 11.59 ± 1.39 MPa to 10.73 ± 1.11 MPa), although the difference was not statistically significant. In agreement with this observation, a reduced ultimate tensile strength was reported for NaOH treated (5 hours in 5 N NaOH) PCL films (12.21 ± 3.38 MPa) and the untreated ones (17.33 ± 4.49 MPa) produced by dichloromethane casting (6% wt/v) and subsequent biaxial stretch [24, 25]. Prolonged treatment in NaOH was not suggested for the modification of the thin polymer films due to the compromising effect to their mechanical strength. Young’s modulus (E , a measurement of stiffness) showed that the PCL/PLA films were significantly more rigid than the homopolymer films. Maximum strain showed that PCL films could be stretched 2–3 times longer than the PCL/PLA films before the point of failure. The elongation at break varied from 650 to 1000%.

The average Young’s modulus for PCL films and NaOH treated PCL films (4 ml of 3% wt/v PCL; $n = 20$) were approximately 115.48 ± 9.95 MPa and 118.89 ± 10.75 MPa, respectively. The slightly increased rigidity for NaOH treated PCL films was speculated to be resulted from the preferential degradation of amorphous part of the polymer against the ordered crystalline structure. However, the difference was not statistically significant.

Table 3 Mechanical properties of PCL films, NaOH treated PCL films, PCL/PLA blend films and NaOH treated blend films

Samples	Max. STR. (MPa)	Max. STN. (mm/mm)	Young's Modulus (MPa)
PCL	16.3 ± 3.97	7.67 ± 2.47	115.48 ± 9.95
PCL (NaOH treated)	14.98 ± 2.77	7.14 ± 1.78	118.89 ± 10.75
PCL/PLA	11.59 ± 1.39	2.86 ± 0.91	175.52 ± 19.46
PCL/PLA (NaOH treated)	10.73 ± 1.10	2.44 ± 0.91	156.48 ± 17.49

Table 4 DSC data, showing melting temperature and crystallinity of different materials

Samples	Melting point T_m (°C)	Enthalpy of fusion ΔH_m (J/g)	Crystallinity χ (%)
PCL pellets	61.53 ± 0.38	79.85 ± 2.61	58.96 ± 1.92
PCL film	57.83 ± 0.29	85.79 ± 5.54	63.35 ± 4.09
PCL-OH film	58.13 ± 0.42	82.48 ± 5.24	60.89 ± 3.87
PLA crystal	70.51 ± 0.05	2.23 ± 1.05	1.64 ± 0.77
PLA film	53.65 ± 0.19	26.09 ± 3.71	1.926 ± 0.27
PCL/PLA film	59.18 ± 0.25	61.53 ± 5.53	45.43 ± 4.07
PCL/PLA-OH film	59.04 ± 0.23	63.63 ± 3.01	46.98 ± 2.22

Enthalpy of fusion was used to calculate the crystallinity, and the enthalpy of fusion (135.44 J/g) of 100% crystallinity (χ) of PCL was used as a reference

3.7 Crystallinity of PCL and PCL/PLA films

PCL films prepared in our lab showed a melting temperature of 57.83°C and a crystallinity of 63.35% (Table 4). This falls in the same range with the value (61%) reported for the crystallinity of pure PCL [26]. NaOH treatment only resulted in slight change in these two thermal properties when compared with the untreated samples; however, when the standard deviation of the crystallinity was considered the data were found to be in the same range. Data for the composite PCL/PLA films showed that incorporation of PLA, an amorphous polymer with low crystallinity (1.64%), significantly reduced the crystallinity to 45.43%. In addition, both PCL and PCL/PLA thin films showed a reduced melting temperature (T_m) than the raw materials.

3.8 Protein adsorption

Protein adsorption analysis (Fig. 6) showed that the porous air surfaces tended to absorb a higher amount of serum proteins than the smoother glass surfaces. However, NaOH treatment did not enhance the capability of the materials to absorb more proteins although it increased the hydrophilicity of the films as described above. Similar protein adsorption was measured for the glass surfaces of both PCL and PCL/PLA films before and after NaOH treatment, which was also found to be comparable to that of tissue culture plastic (TCP).

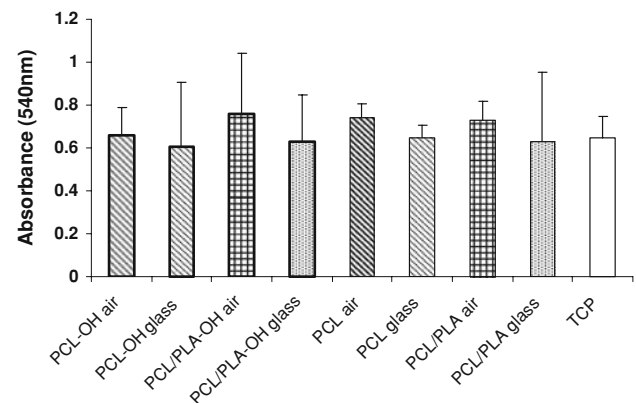


Fig. 6 BCA protein adsorption analysis for different materials, showing that the porous air surfaces tended to absorb more proteins than the relatively smooth glass surface. NaOH treatment didn't affect protein adsorption to the surface. The amount of proteins adsorbed onto both the glass surfaces and the air surfaces was comparable to that on the tissue culture plastic (TCP). PCA represents PCL/PLA blend and -OH indicates NaOH treatment

4 Discussion

A good material for nerve tubulization should have the following features: (a) biocompatible, (b) thin and flexible, (c) bioresorbable, (d) inhibitory to processes causing pathology, (e) beneficial to processes contributing to healing and regeneration [5]. Several other important properties that nerve guidance tubes should possess are: easily fabricated with the desired dimensions and topography, implanted with

relative ease, sterilisable, pliable enough to glide and bend *in vivo* and stiff enough not to collapse *in situ* [27]. The ideal material should also be non-immunogenic, causing neither local tissue irritation nor allergic response [28] and be stable as long as the regeneration is in progress and decompose rather than being removed once the repairing is completed to avoid the risk of injuring the repaired nerve [29]. The incorporation of supportive cells, an internal oriented matrix, intraluminal channels to mimic the structure of nerve fascicles, and electrical activities are also essential features for optimal nerve guidance [30].

PCL films and PCL/PLA polymer blend films possess almost all of the properties mentioned above. They can be readily rolled up to form tubes by wrapping around a mandrel of a decided size and heat sealed without using any toxic chemicals. Supportive cells and/or growth factors suspended in transport matrices can be delivered through the end of the tubes once they are sutured in place. The blend system also provides the potential for modifying the mechanical properties and degradation rate of the films by adjusting the molecular weight and composition of the two polymers. PLA of low molecular weight absorbs water and swells in physiological solutions due to the higher hydrophilic end-groups density [31], which is detrimental to regenerating nerve. PLA of high molecular weight, however, is associated with longer degradation. In this study, the polymer blend consisting of PLA ($M_n \sim 30,000$) and PCL ($M_n \sim 80,000$) in the ratio of 1:4 showed no sign of swelling after 6 months in phosphate buffered saline.

4.1 Higher tensile strength than fresh rat sciatic nerve

Tensile strength is a crucial physical parameter of a good nerve conduit; however, little work has been done to find the standard reference value for an ideal nerve conduit. In addition, no direct comparison could be made due to the variance of fabrication techniques and the machinery systems adopted in individual work. However, the tensile strength for PCL films (16.3 MPa and 14.98 MPa before and after NaOH treatment) and PCL/PLA blend films (11.59 MPa and 10.73 MPa before and after NaOH treatment) fell in the same range (10.9 MPa) as the PCL membranes cast using methylene chloride (i.e. dichloromethane) with a thickness of 120 μm [32]. These values are significantly higher than the tensile strength measured for fresh F344 rat sciatic nerve (2.72 MPa) [33].

4.2 Thin walled conduits

Nerve conduits with thick walls are more rigid and will subsequently result in encumbered handle-ability and poor *in vivo* compatibility with local tissues. For example, poly-[bis-(ethylalanate)-phosphazene] conduit prepared using

dip-coating had a wall thickness of 500 μm , which made it difficult to insert the suture threads under the operating microscope [34]. In a recent work, poly-D,L-lactide conduit produced by dip-coating around a poly-(vinyl alcohol) (PVA) rod was used to test the influence of wall thickness on nerve regeneration. It was reported that regenerated axons were significantly longer in conduits with a wall thickness of 0.81 mm when compared with that in conduits with thicker walls of 1.10 mm, 1.28 mm and 1.44 mm [35].

Meek et al. [36, 37] suggested that the idea behind the successful use of a thin-walled nerve guide is less biomaterial and less swelling. Conduits with thin walls were associated with less neuroma formation both proximal and distal to the tube, which was attributed to the greater elasticity of the thin walls [38]. This ultra thin feature of the solvent-cast PCL and PCL/PLA films rendered these materials highly flexible and as such could avoid the compression and irritation to surrounding tissues once implanted. In addition, this micro-thin film means less allogenic biological material will be released and hence will invoke minimal adverse host-tissue response [32]. Physically, decreased crystallinity and spherulite size have been observed when the thickness of PCL films decreases since nucleation and crystallization are slower in thin films due to decreased molecular mobility [39].

To date, no nerve conduit with a thickness of less than 100 μm has been reported for peripheral nerve repair. Small wall thickness can result in the collapsing of the device *in vivo* using other materials. For example, amorphous poly (DLA- ϵ -CL) with a thickness of 170 μm collapsed 26 weeks postoperatively [40]. 40% of the nerve conduits made of electrospun PCL/PLGA fibres with a thickness of 155 μm collapsed 4 months after surgery [41]. The robust mechanical properties of PCL and PCL/PLA films could potentially overcome this problem once implanted.

4.3 Increased hydrophilicity and degradation rate and reduced surface roughness after NaOH treatment

Surface wettability is an important property of a biomaterial and should be taken into account when biocompatibility with cells is analyzed. A cell attachment study carried out recently by Wei and co-workers confirmed that the more hydrophilic the surface, the more fibroblasts adhered in the initial stage. Moreover, cells spread much more widely on the hydrophilic surfaces than on the hydrophobic surfaces [42].

Polyester degradation occurs by polymer chain scission, the hydrolytic effect of NaOH treatment accelerates the degradation by introducing random scission to the polymer chains. Therefore, pre-treatment of the films will increase the degradation of polyester-based materials *in vivo*.

NaOH treatment was believed to be able to reduce the polymer surface feature dimensions from micro-scale to nano-scale for both PCL and PLGA films [43–45]. Average surface roughness (R_a) was reduced by nano-metre scale for both PCL and the PCL/PLA films following NaOH treatment, although no visible changes could be detected on the AFM images, this could be due to the porous structure that blocked the effect of NaOH treatment on surface morphology change.

4.4 Porous surface

Porous surface texture can expedite the degradation of PCL. It has been reported that small pits resulting from solvent vaporization are the initiation sites for degradation which further grow into hemispherical holes [46]. High porosity of the PCL films (average 51.0%) produced in this study was speculated to be able to accelerate polymer degradation, together with smaller device size, reactive hydrolytic groups in the backbone, and hydrophilic end groups generated by NaOH treatment [12].

The sparsely distributed penetrating holes make the PCL and PCL/PLA films semi-permeable. Many tissue engineering constructs use porous or mesh-like polymeric matrices since the permeability of nerve guides is of great importance to nerve repair especially for the repair of long nerve gaps. Permeable scaffolds allow the inward diffusion of externally generated growth factors and the outward diffusion of waste products; whereas impermeable conduits can positively affect nerve repair by insulating the area of regeneration, preventing the formation of scar tissue, and by containing the internally generated growth factors inside [47]. Semi-permeable tube wall may also facilitate the formation of the supportive fibrin cable by allowing the inward diffusion of extraneural wound-healing factors [48] and by avoiding the building up of pressure resulting from fluid retention [49]. Improved nerve regeneration and reinnervation have been shown to occur in semi-permeable nerve conduits when compared with impermeable ones [49–52], although controversial results were also reported by other researchers [53–55].

On the other hand, the reparative process of axons within a nerve guide is often accompanied by undesirable escape of regenerating axons out of the neural sheath. In such cases, diminished sensory or motor recovery could happen due to the reduced total number of axons reaching the distal stump [56]. In addition, the escape of regenerating axons may lead to the formation of neuroma, which could cause pain and tenderness at the repair site [57]. The novel semi-permeable structure of films produced in our work will potentially enclose the elongating axons inside the sheath due to the small

size and low percentage of the penetrating holes. The unique property of this material may also prevent the in-growth of fibrous tissue.

4.5 Reduced crystallinity in composite material

PCL of low molecular weight often has high crystallinity and it is crystallinity that controls the biodegradation rate of polymers rather than molecular weight [58, 59]. Modification of the crystalline structure of polymers by blending them with either amorphous or other crystalline polymers has been proven to be able to produce new materials with better properties in terms of degradability, mechanical strength and the ease for suturing during implantation [60]. For example, the crystallization rates of PCL were found markedly reduced in polymer blends comprising poly (ϵ -caprolactone) (PCL) and amorphous poly (vinyl methyl ether) (PVME) as compared to neat PCL [61]. In the present study, the introduction of amorphous PLA reduced the crystallinity of the resultant polymer blend from 63.35% to 45.43%. Since fluid ingress and subsequent hydrolytic chain scission are restricted in the crystalline regions of polymers, faster resorption of polymer scaffold could be envisaged.

4.6 Increased protein adsorption on porous surface

“Cell interactions with foreign surface include four steps: (1) protein adsorptions; (2) cells anchored to adsorbed protein via cell integrins; (3) cell differentiate, multiply, communicate with other cell types and organize themselves; (4) cells and tissues respond to mechanical forces” [62]. Protein adsorption occurs before cells arrive and what the cells interact with is primarily the protein layer rather than the actual surface of the biomaterial. Extracellular matrix (ECM) proteins would non-specifically adsorb on a biomaterial when it is introduced into the body and the interaction of biomaterial with cells would be through these ECM proteins. In this study, increased surface hydrophilicity didn’t increase the amount of protein absorbed. This is in contradiction to the report that increased surface wettability is believed to be associated with enhanced protein adsorption and will consequently encourage cell adhesion of anchorage-dependent cells [63, 64]. However, hydrophilicity is not the only factor that affects protein adsorption, other physicochemical properties of the biomaterial at the interface, such as charge or polarity as well as its roughness and degree of heterogeneity in the distribution of reactive chemical groups are all responsible for the selectivity of proteins absorbed onto substrate surface [65].

5 Conclusions

We have developed a method for producing novel ultra-thin polymer-based PCL and PCL/PLA blend films as a promising scaffold for peripheral nerve repair. The micro-porous air surface showed enhanced protein adsorption and was hypothesized to increase the adhesion of nerve cells and glial cells. NaOH treatment reduced the surface roughness and increased the hydrophilicity of the materials which are favourable for cell attachment and proliferation. NaOH modification and the incorporation of fast degrading PLA were speculated to accelerate the in vivo degradation of the PCL/PLA blend material. To our knowledge, this is the first time a nerve conduit with a wall thickness of less than 100 μm has been produced with the desired flexibility and mechanical strength for clinical handling and in vivo stability. A conduit wall comprising a plurality of layers of film can be applied to injury sites that require prolonged protection and guidance without compromising the flexibility of the material.

The nerve conduits developed in the present study are easy to sterilize, low cost and non-toxic. Other desirable properties include excellent handleability by surgeons and immediate availability for clinical operation. Importantly, this purely synthetic product can avoid all inherited problems associated with animal products.

Acknowledgements This work is funded by Engineering and Physical Sciences Research Council (EPSRC). The authors would like to thank the technical staff at School of Materials for their kind assistance.

References

1. A.B. Dagum, Peripheral nerve regeneration, repair, and grafting. *J. Hand Ther.* **11**, 111 (1998)
2. P.N. Mohanna, R.C. Young, M. Wiberg, G. Terenghi, A composite poly-hydroxybutyrate-glia growth factor conduit for long nerve gap repairs. *J. Anat.* **203**, 553 (2003). doi:10.1046/j.1469-7580.2003.00243.x
3. S.E. Mackinnon, A.L. Dellon, in *Surgery of the Peripheral Nerve. Nerve Repair and Nerve Grafting* (Thieme Medical Publishers, New York, 1988), pp. 89–129
4. M.F. Meek, W.F.A. Den Dunnen, J.M. Schakenraad, P.H. Robinson, Evaluation of functional nerve recovery after reconstruction with a poly (DL-Lactide- ϵ -Caprolactone) nerve guide, filled with modified denatured muscle tissue. *Microsurgery* **17**, 555 (1996). doi:10.1002/(SICI)1098-2752(1996)17:10<555::AID-MICR5>3.0.CO;2-P
5. R.D. Fields, J.M. Le Beau, F.M. Longo, M.H. Ellisman, Nerve regeneration through artificial tubular implants. *Prog. Neurobiol.* **33**, 87 (1989). doi:10.1016/0301-0082(89)90036-1
6. C.E. Schmidt, J.B. Leach, Neural tissue engineering: strategies for repair and regeneration. *Annu. Rev. Biomed. Eng.* **5**, 293 (2003). doi:10.1146/annurev.bioeng.5.011303.120731
7. R.S. Bezwada, D.D. Jamiolkowski, I.Y. Lee, V. Agarwal, J. Persivale, S. Trenka-Benthin, M. Erneta, J. Suryadevara, A. Yang, S. Liu, Monocryl® suture, a new ultra-pliant absorbable monofilament suture. *Biomaterials* **16**, 1141 (1995). doi:10.1016/0142-9612(95)93577-Z
8. P.D. Darney, S.E. Monroe, C.M. Klaisle, A. Alvarado, Clinical evaluation of the Capronor contraceptive implant: preliminary report. *Am. J. Obstet. Gynecol.* **160**, 1292 (1989)
9. S. Dumitriu, *Polymeric Biomaterials*, 2nd edn. rev. (Marcel Dekker Inc., New York, 2001), pp. 95–97, 107–109, 402, 403
10. S.C. Woodward, P.S. Brewer, F. Moatamed, A. Schindler, C.G. Pitt, The intracellular degradation of poly (ϵ -caprolactone). *J. Biomed. Mater. Res.* **19**, 437 (1985). doi:10.1002/jbm.820190408
11. H. Kweon, M.K. Yoo, I.K. Park, T.H. Kim, H.C. Lee, H.S. Lee, J.S. Oh, T. Akaike, C.S. Cho, A novel degradable polycaprolactone networks for tissue engineering. *Biomaterials* **24**, 801 (2003). doi:10.1016/S0142-9612(02)00370-8
12. G. Chouzouri, M. Xanthos, In vitro bioactivity and degradation of polycaprolactone composites containing silicate fillers. *Acta Biomater.* **3**, 745 (2007). doi:10.1016/j.actbio.2007.01.005
13. P.H. Robinson, B. van der Lei, H.J. Hoppen, J.W. Leenslag, A.J. Pennings, P. Nieuwenhuis, Nerve regeneration through a two-ply biodegradable nerve guide in the rat and the influence of ACTH₄₋₉ nerve growth factor. *Microsurgery* **12**, 412 (1991). doi:10.1002/micr.1920120608
14. M.E. Broz, D.L. VanderHart, N.R. Washburn, Structure and mechanical properties of poly (D, L-lactic acid)/poly(ϵ -caprolactone) blends. *Biomaterials* **24**, 4181 (2003). doi:10.1016/S0142-9612(03)00314-4
15. R.L. Reis, A.M. Cunha, Characterization of two biodegradable polymers of potential application within the biomaterials field. *J. Mater. Sci. Mater. Med.* **6**, 786 (1995). doi:10.1007/BF00134318
16. J. Spěvák, J. Brus, T. Divers, Y. Grohens, Solid-state NMR study of biodegradable starch/polycaprolactone blends. *Eur. Polym. J.* **43**, 1866 (2007). doi:10.1016/j.eurpolymj.2007.02.021
17. R. Dell'Erba, G. Groeninckx, G. Maglio, M. Malinconico, A. Migliozi, Immiscible polymer blends of semicrystalline biocompatible components: thermal properties and phase morphology analysis of PLLA/PCL blends. *Polymer (Guildf)* **42**, 7831 (2001). doi:10.1016/S0032-3861(01)00269-5
18. L. Wang, W. Ma, R.A. Gross, S.P. McCarthy, Reactive compatibilization of biodegradable blends of poly (lactic acid) and poly (ϵ -caprolactone). *Polym. Degrad. Stab.* **59**, 161 (1998). doi:10.1016/S0141-3910(97)00196-1
19. P.N. Mohanna, G. Terenghi, M. Wiberg, Composite PHB-GGF conduit for long nerve gap repair: a long-term evaluation. *J. Plast. Reconstr. Surg. Hand Surg.* **39**, 129 (2005). doi:10.1080/02844310510006295
20. D.F. Kalbermatten, P.J. Kingham, D. Mahay, C. Mantovani, J. Pettersson, W. Raffoul, H. Balcin, G. Pierer, G. Terenghi, Fibrin matrix for suspension of regenerative cells in an artificial nerve conduit. *J. Plast. Reconstr. Aesthet. Surg.* **61**, 669 (2008). doi:10.1016/j.bjps.2007.12.015
21. V. Crescenzi, G. Manzini, G. Calzolari, C. Borri, Thermodynamics of fusion of poly β -propiolactone and poly ϵ -caprolactone. Comparative analysis of the melting of aliphatic polylactone and polyester chains. *Eur. Polym. J.* **8**, 449 (1972). doi:10.1016/0014-3057(72)90109-7
22. T. Freier, C. Kunze, K.-P. Schmitz, Solvent removal from solution-cast films of biodegradable polymers. *J. Mater. Sci. Lett.* **20**, 1929 (2001). doi:10.1023/A:1013174400236
23. M. Sun, S. Downes, Solvent-cast PCL films support the regeneration of NG108-15 nerve cells. in *International Conference on Smart Materials and Nanotechnology in Engineering. Proceedings of the SPIE vol. 6423*, p. 64230, July 2007
24. M.S.K. Chong, C.N. Lee, S.H. Teoh, Characterization of smooth muscle cells on poly (ϵ -caprolactone) films. *Mater. Sci. Eng. C* **27**, 309 (2007). doi:10.1016/j.msec.2006.03.008

25. L.P.K. Ang, Z.Y. Cheng, R.W. Beuerman, S.H. Teoh, X. Zhu, D.T.H. Tan, The development of a serum-free derived bioengineered conjunctival epithelial equivalent using an ultrathin poly (ϵ -caprolactone) membrane substrate. *Invest. Ophthalmol. Vis. Sci.* **47**, 105 (2006). doi:[10.1167/iov.05-0512](https://doi.org/10.1167/iov.05-0512)
26. S.J. Huang, in *Encyclopedia of Polymer Science and Engineering*, vol. 2, ed. by H.F. Mark, N. Bikales, C.G. Overberger, G. Menges (Wiley, New York, 1985)
27. F.C. Bragança, D.S. Rosa, Thermal, mechanical and morphological analysis of poly(ϵ -caprolactone), cellulose acetate and their blends. *Polym. Adv. Technol.* **14**, 669 (2003). doi:[10.1002/pat.381](https://doi.org/10.1002/pat.381)
28. T.W. Hudson, G.R. Evans, C.E. Schmidt, Engineering strategies for peripheral nerve repair. *Clin. Plast. Surg.* **26**, 617 (1999)
29. V.B. Doolabh, M.C. Hertl, S.E. Mackinnon, The role of conduits in nerve repair: a review. *Rev. Neurosci.* **7**, 47 (1996)
30. W.F.A. den Dunnen, I. Stokroos, E.H. Blaauw, A. Holwerda, A.J. Pennings, P.H. Robinson, J.M. Schakenraad, Light-microscopic and electronmicroscopic evaluation of short-term nerve regeneration using a biodegradable poly (DL-lactide- ϵ - caprolactone) nerve guide. *J. Biomed. Mater. Res.* **31**, 105 (1996). doi:[10.1002/\(SICI\)1097-4636\(199605\)31:1<105::AID-JBM13>3.0.CO;2-M](https://doi.org/10.1002/(SICI)1097-4636(199605)31:1<105::AID-JBM13>3.0.CO;2-M)
31. Y.-C. Huang, Y.-Y. Huang, Biomaterials and strategies for nerve regeneration. *Artif. Organs* **30**, 514 (2006). doi:[10.1111/j.1525-1594.2006.00253.x](https://doi.org/10.1111/j.1525-1594.2006.00253.x)
32. Q. Cai, J. Bei, S. Wang, In vitro study on the drug release behaviour from polylactide-based blend matrices. *Polym. Adv. Technol.* **13**, 534 (2002). doi:[10.1002/pat.222](https://doi.org/10.1002/pat.222)
33. K.S. Tiaw, S.H. Teoh, R. Chen, M.H. Hong, Processing methods of ultrathin poly(ϵ -caprolactone) films for tissue engineering applications. *Biomacromolecules* **8**, 807 (2007). doi:[10.1021/bm060832a](https://doi.org/10.1021/bm060832a)
34. G.H. Borschel, K.F. Kia Jr., W.M. Kuzon, R.G. Dennis, Mechanical properties of acellular peripheral nerve. *J. Surg. Res.* **114**, 133 (2003). doi:[10.1016/S0022-4804\(03\)00255-5](https://doi.org/10.1016/S0022-4804(03)00255-5)
35. N. Nicoli Aldini, M. Fini, M. Rocca, G. Giavaresi, R. Giardino, Guided regeneration with resorbable conduits in experimental peripheral nerve injuries. *Int. Orthop. SICOT* **24**, 121 (2000). doi:[10.1007/s002640000142](https://doi.org/10.1007/s002640000142)
36. G.E. Rutkowski, C.A. Heath, Development of a bioartificial nerve graft. II. Nerve regeneration in vitro. *Biotechnol. Prog.* **18**, 373 (2002). doi:[10.1021/bp020280h](https://doi.org/10.1021/bp020280h)
37. M.F. Meek, W.F.A. den Dunnen, H. Bartels, P.H. Robinson, J.M. Schakenraad, Peripheral nerve regeneration and functional nerve recovery after reconstruction with thin-walled biodegradable poly (DL-lactide- ϵ -caprolactone) nerve guides. *Cell Mater.* **7**, 53 (1997)
38. M.F. Meek, P.H. Robinson, I. Stokroos, E.H. Blaauw, G. Kors, W.F.A. den Dunnen, Electronmicroscopical evaluation of short-term nerve regeneration through a thin-walled biodegradable poly (DLA- ϵ -CL) nerve guide filled with modified denatured muscle tissue. *Biomaterials* **22**, 1177 (2001). doi:[10.1016/S0142-9612\(00\)00340-9](https://doi.org/10.1016/S0142-9612(00)00340-9)
39. T.B. Ducker, G.J. Hayes, Experimental improvements in the use of silastic cuff for peripheral nerve repair. *J. Neurosurg.* **28**, 582 (1968)
40. D. Simon, A. Holland, R. Shanks, Poly (caprolactone) thin film preparation, morphology, and surface texture. *J. Appl. Polym. Sci.* **103**, 1287 (2007). doi:[10.1002/app.25228](https://doi.org/10.1002/app.25228)
41. M.F. Meek, W.F. den Dunnen, J.M. Schakenraad, P.H. Robinson, Long-term evaluation of functional nerve recovery after reconstruction with a thin-walled biodegradable poly (DL-Lactide- ϵ -caprolactone) nerve guide, using walking track analysis and electrostimulation tests. *Microsurgery* **19**, 247 (1999). doi:[10.1002/\(SICI\)1098-2752\(1999\)19:5<247::AID-MICR7>3.0.CO;2-E](https://doi.org/10.1002/(SICI)1098-2752(1999)19:5<247::AID-MICR7>3.0.CO;2-E)
42. S. Panseri, C. Cunha, J. Lowery, U.D. Carro, F. Taraballi, S. Amadio, A. Vescovi, F. Gelain, Electrospun micro- and nanofiber tubes for functional nervous regeneration in sciatic nerve transections. *BMC Biotechnol.* **8**, 39 (2008). doi:[10.1186/1472-6750-8-39](https://doi.org/10.1186/1472-6750-8-39)
43. J. Wei, Y. Masao, T. Shinji, H. Masayuki, K. Eiji, B. Liu, O. Yutaka, Adhesion of mouse fibroblasts on hexamethyldisiloxane surfaces with wide range of wettability. *J. Biomed. Mater. Res.* **81**, 66 (2007). doi:[10.1002/jbm.b.30638](https://doi.org/10.1002/jbm.b.30638)
44. A. Thapa, T.J. Webster, K.M. Haberstroh, Polymers with nano-dimensional surface features enhance bladder smooth muscle cell adhesion. *J. Biomed. Mater. Res.* **67A**, 1374 (2003). doi:[10.1002/jbm.a.20037](https://doi.org/10.1002/jbm.a.20037)
45. A. Thapa, T.J. Webster, K.M. Haberstroh, Nano-structured polymers enhance bladder smooth muscle cell function. *Biomaterials* **24**, 2915 (2003). doi:[10.1016/S0142-9612\(03\)00123-6](https://doi.org/10.1016/S0142-9612(03)00123-6)
46. R.J. Vance, D.C. Miller, A. Thapa, K.M. Haberstroh, T.J. Webster, Decreased fibroblast cell density on chemically degraded poly-lactic-co-glycolic acid, polyurethane, and polycaprolactone. *Biomaterials* **25**, 2095 (2004). doi:[10.1016/j.biomaterials.2003.08.064](https://doi.org/10.1016/j.biomaterials.2003.08.064)
47. H. Nishida, Y. Tokiwa, Confirmation of colonization of degrading bacterium strain SC-17 on poly(3-hydroxybutyrate) cast film. *J. Environ. Polym. Degrad.* **3**, 187 (1995). doi:[10.1007/BF02068673](https://doi.org/10.1007/BF02068673)
48. C.L.A.M. Vleggeert-Lankamp, G.C.W. de Ruyter, J.F.C. Wolfs, A.P. Pêgo, R.J. van den Berg, H.K.P. Feirabend, M.J.A. Malessy, E.A.J.F. Lakke, Pores in synthetic nerve conduits are beneficial to regeneration. *J. Biomed. Mater. Res.* **80A**, 965 (2006). doi:[10.1002/jbm.a.30941](https://doi.org/10.1002/jbm.a.30941)
49. F.J. Rodriguez, N. Gomez, G. Perego, X. Navarro, Highly permeable polylactide-caprolactone nerve guides enhance peripheral nerve regeneration through long gaps. *Biomaterials* **20**, 1489 (1999). doi:[10.1016/S0142-9612\(99\)00055-1](https://doi.org/10.1016/S0142-9612(99)00055-1)
50. A.P. Pêgo, A.A. Poot, D.W. Grijpma, J. Feijen, Copolymers of trimethylene carbonate and ϵ -caprolactone for porous nerve guides: synthesis and properties. *J. Biomater. Sci. Polym. Ed.* **12**, 35 (2001). doi:[10.1163/156856201744434](https://doi.org/10.1163/156856201744434)
51. B.G. Uzman, G.M. Villegas, Mouse sciatic nerve regeneration through semipermeable tubes: a quantitative model. *J. Neurosci. Res.* **9**, 325 (1983). doi:[10.1002/jnr.490090309](https://doi.org/10.1002/jnr.490090309)
52. C.-B. Jenq, R.E. Coggeshall, Permeable tubes increase the length of the gap that regenerating axons can span. *Brain Res.* **408**, 239 (1987). doi:[10.1016/0006-8993\(87\)90379-9](https://doi.org/10.1016/0006-8993(87)90379-9)
53. P. Aebischer, V. Guénard, S.R. Winn, R.F. Valentini, P.M. Galletti, Blind-ended semipermeable guidance channels support peripheral nerve regeneration in the absence of a distal nerve stump. *Brain Res.* **454**, 179 (1988). doi:[10.1016/0006-8993\(88\)90817-7](https://doi.org/10.1016/0006-8993(88)90817-7)
54. B. Knoops, H. Hurtado, P. van den Bosch de Aguilar, Rat sciatic nerve regeneration within an acrylic semipermeable tube and comparison with a silicone impermeable material. *J. Neuropathol. Exp. Neurol.* **49**, 438 (1990)
55. K.L. Gibson, L. Remson, A. Smith, N. Satterlee, G.M. Strain, J.K. Daniloff, Comparison of nerve regeneration through different types of neural prostheses. *Microsurgery* **12**, 80 (1991). doi:[10.1002/micr.1920120205](https://doi.org/10.1002/micr.1920120205)
56. R.D. Keeley, K.D. Nguyen, M.J. Stephanides, J. Padilla, J.M. Rosen, The artificial nerve graft: a comparison of blended elastomerhydrogel with polyglycolic acid conduits. *J. Reconstr. Microsurg.* **7**, 93 (1991). doi:[10.1055/s-2007-1006766](https://doi.org/10.1055/s-2007-1006766)
57. M. Siemionow, A. Sari, A contemporary overview of peripheral nerve research from the Cleveland Clinic Microsurgery Laboratory. *Neurol. Res.* **26**, 218 (2004). doi:[10.1179/016164104225013860](https://doi.org/10.1179/016164104225013860)
58. A.J. Vernadakis, H. Koch, S.E. Machinnon, Management of neuromas. *Clin. Plast. Surg.* **30**, 247 (2003). doi:[10.1016/S0094-1298\(02\)00104-9](https://doi.org/10.1016/S0094-1298(02)00104-9)

59. H.M. Shabana, R.H. Olley, D.C. Bassett, B. Jungnickel, Phase separation induced by crystallization in blends of polycaprolactone and polystyrene: an investigation by etching and electron microscopy. *J. Polym.* **41**, 5513 (2000). doi:[10.1016/S0032-3861\(99\)00713-2](https://doi.org/10.1016/S0032-3861(99)00713-2)
60. C.S. Ng, S.H. Teoh, T.S. Chung, D.W. Hutmacher, Simultaneous biaxial drawing of poly (ϵ -caprolactone) films. *Polymer (Guildf)* **41**, 5855 (2000). doi:[10.1016/S0032-3861\(99\)00760-0](https://doi.org/10.1016/S0032-3861(99)00760-0)
61. R.J. Müller, I. Kleeger, W.D. Decker, Biodegradation of polyesters containing aromatic constituents. *J. Biotechnol.* **86**, 87 (2001). doi:[10.1016/S0168-1656\(00\)00407-7](https://doi.org/10.1016/S0168-1656(00)00407-7)
62. W.Y. Yam, J. Ismail, H.W. Kammer, H. Schmidt, C. KummerlÖwe, Polymer blends of poly (ϵ -caprolactone) and poly (vinyl methyl ether)-thermal properties and morphology. *Polymer (Guildf)* **40**, 5545 (1999). doi:[10.1016/S0032-3861\(98\)00807-6](https://doi.org/10.1016/S0032-3861(98)00807-6)
63. B.D. Ratner, A.S. Hoffman, F.J. Schoen, *Biomaterials Science: An introduction to Materials in Medicine*, 2nd edn. (Elsevier Inc., Amsterdam, 2004), pp. 67–80
64. D.L. Mooradian, P. Trescony, K. Keeney, L.T. Furcht, Effect of glow discharge surface modification of plasma TFE vascular graft material on fibronectin and laminin retention and endothelial cell adhesion. *J. Surg. Res.* **53**, 74 (1992). doi:[10.1016/0022-4804\(92\)90016-S](https://doi.org/10.1016/0022-4804(92)90016-S)
65. J.G. Steele, C. McFarland, B.A. Dalton, G. Johnson, M.D.M. Evans, C.R. Howlett, P.A. Underwood, Attachment of human-derived bone cells to tissue culture polystyrene and to unmodified polystyrene: the effect of surface chemistry upon initial cell attachment. *J. Biomater. Sci. Polym. Ed.* **5**, 245 (1993). doi:[10.1163/156856293X00339](https://doi.org/10.1163/156856293X00339)